Effect of sliding velocity on friction-induced microstructural evolution in Copper

Grégoire Jacquet Jacquet, Guillaume Kermouche, Cédric Courbon, David Tumbajoy-Spinel, Joel Rech

Effect of sliding velocity on friction-induced microstructural evolution in Copper

G Jacquet[1,2,*], G Kermouche[1], C Courbon[2], D Tumbajoy[1,2] and J Rech[2]

[1] Ecole des Mines de Saint-Etienne, Centre SMS, Laboratoire LGF, CNRS UMR 5307, 158 Cours Fauriel, 42023 Saint-Etienne, France
[2] Ecole Nationale d'Ingénieurs de Saint-Etienne, LTDS, CNRS UMR 5513, 58 Rue Jean Parot, 42023 Saint-Etienne, France
* E-mail: jacquet@emse.fr

Abstract: Durability of engineering workpieces surfaces is well-known to be strongly related to the microstructural evolutions induced by machining processes. One current challenge is to choose the right process parameters, such as the sliding speed, in order to optimize both the subsurface microstructure and the surface properties. In this paper, a special tribometer, able to simulate contact pressures and cutting speeds occurring during machining, has been used to characterize the effect of sliding velocity on microstructural evolution induced in copper. Significant recrystallization and grain refinement phenomena have been observed for the highest sliding speed tested (250m/min). Finite element analysis have been performed to extract local variables near the pin/copper bar interface. A good agreement is noticed between the equivalent plastic strain level, the temperature rise, the resulting grain size and the hardness gradient.

1. Introduction

Nowadays, a significant part of the functional surfaces is still created by mechanical engineering processes, such as cutting or superfinishing. One of the most important parameter influencing the engineering surface overall quality is the cutting (sliding) speed, which can lead to severe thermo-mechanical loadings and thus modify the resulting surface integrity [1-3]. Although most of the papers on surface integrity deal with the residual stress field [4-6], it shall not be omitted that the surface microstructure evolution may also play a significant role on the durability of engineering workpieces [7-9]. A current challenge, both academic and industrial, is to predict these microstructure evolutions and their consequences on the surface properties (wear, hardness, fretting fatigue) in order to identify the best cutting parameters.

Similarly to standard thermomechanical treatments (forging, rolling...) the way the microstructures are modified by machining processes is strongly related to stress, strain, strain rate and temperature paths [10-11]. Thanks to finite element analyses, it is now possible to estimate with good accuracy these data for scholar experimental cases (orthogonal cutting, high speed sliding). However it assumes that the thermomechanical properties of the investigated material have been fully identified in the appropriate strain, strain rate and temperature range.

In this paper, we investigate the microstructure evolution in a commercially pure copper induced by a high speed tribometer initially designed to measure the friction coefficients for cutting applications [12]. This scholar test has been chosen because it depends mainly on two parameters (sliding speed and load).

Copper was chosen because a significant amount of data can be found in the literature that could be applied in the context of severe plastic deformation (SPD) occurring during machining processes: superfinish turning tests[13,14], accumulative roll bonding tests [15], multiple compression tests [16], plane strain machining tests [17], dry machining tests [18]...

Moreover, copper is a metal with low stacking fault energy, meaning that the movement of dislocations is not easy and recovery mechanisms (formation of sub-boundaries, annihilation of dislocations by pairs) have low efficiency [19,20]. During hot deformation, a mechanism of discontinuous dynamic recrystallization (DDRX) is expected: nucleation and growth of new grains. On the other hand, at low temperature, SPD can lead to the formation of new ultrafine grains. In fact, when strain increases, accumulation of dislocations within sub-boundaries increase their misorientations leads to their progressive transformations in grains boundaries, as shown by [21]. Temperature at the surface of the work material is thus a key parameter, since it has a strong influence on the kind of mechanism involved during friction test.

In the first part of this paper, the high speed tribometer and the related finite element model are detailed. Effect of sliding velocity on experimental and numerical results is presented in part 4, and discussed in part 5. A conclusion is finally brought on the potential of this test to understand the microstructural modifications induced by machining processes.

2. Material and methods

Commercially pure copper bar with a 40mm diameter has a microstructure with an initial average grain size of about 50µm (Figure 1).

Figure 1: Optical micrograph showing the initial microstructure of the copper bar.
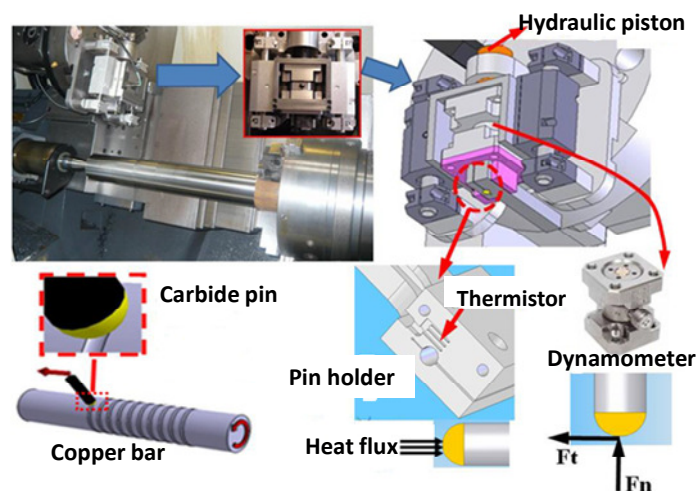

Figure 2: Experimental device used to perform sliding tests.

The copper bar is mounted on a CNC lathe and is in rotation during the test (Figure 2). The macroscopic sliding velocity (V_s) is controlled by the rotation speed of the bar. A Ø9mm spherical pin, fixed into a pin holder, generates friction. A predetermined feed per revolution of 1.8mm avoid the pin from always sliding on the same part of the bar. It is important to note that each friction test is performed during a time long enough to reach stationary friction and thermal conditions as shown in [12]. During a test the desired normal force (F_n) is generated by a hydraulic piston. A dynamometer, fixed on the pin holder, measures the normal and tangential (F_t) forces. Then, the macroscopic friction coefficient is obtained by the following ratio:

$$\mu_{mac} = \frac{F_t}{F_n} \tag{1}$$

Moreover, a thermistor, located very close to the spherical face of the pin, records the temperature. By an inverse method presented in [12], the heat flux transmitted to the pin (ϕ_{pin}) is estimated. This flux corresponds only for a part of the total energy (ϕ_{tot}) dissipated during the test, given that a large fraction of the heat (α) remains in the copper (ϕ_{copper}). ϕ_{tot} is the product of the tangential force and the macroscopic sliding velocity.

$$\phi_{tot} = F_t V_s \tag{2}$$

$$\alpha = \frac{\phi_{copper}}{\phi_{tot}} \tag{3}$$

The influence of sliding velocity on global (μ_{mac}, α) and local (ε, T, etc.) variables and therefore on microstructural evolution in copper has been investigated with an applied normal force $F_n = 600N$. The sliding velocity V_s is defined as the tangential component of the velocity, due to the rotation of the copper bar. Studied values of V_s are 20, 100 and 250 m/min and the revolutions per minute (rpm) associated are 163, 816 and 2040, respectively. The translation of the pin generated a normal component (0.3, 1.5 and 3.7 m/min respectively) which has been neglected since it represented less than 2% of macroscopic sliding velocity. Before each friction test, a new pin was used and a cutting tool refreshed the surface of the copper bar affected by the pin. Samples were extracted from the bar, polished, and then observed in the plane perpendicular to the sliding direction (Figure 3) with Scanning Electron Microscopes (SEM) Jeol© 6500F and Zeiss© Supra 55VP using two different methods:

1- Images obtained by orientation contrast of Backscattered Electrons (BSE). They permit to have statistical information about the microstructure evolution. Presence of recrystallized grains or not, depth of affected layers...
2- Maps obtained by Electron Backscattered Diffraction (EBSD) method. They gave us information about local texture, misorientation of grain boundaries, accurate grain size...

Moreover, for some samples, a nanoindenter NHT, produced by CSM Instruments SA© has been used to characterize evolution of hardness in function of depth under the surface. As shown in Figure 4, 225 indentation tests were performed with a diamond Berckovich indenter, following a square grid configuration, with 10μm between each print. The indentation force was 10mN with a loading and uploading rate of 20mN/min.
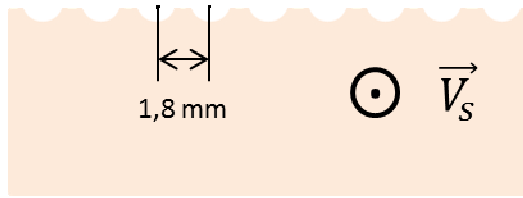
Figure 3: schematic representation of samples used for characterization with SEM.
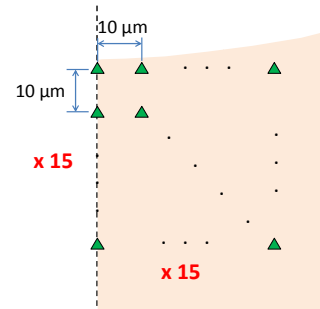

Figure 4: procedure used for nanoindentation tests.

3. Numerical Simulations

μ_{mac} and ϕ_{pin} are macroscopic data directly obtained after friction tests. The model initiated by Bonnet [22] and Zemzemi [23], and completed by Courbon [24], focus on describing local phenomena occurring at the pin/work piece interface. In term of friction coefficient, the macroscopic one μ_{mac} is not the relevant parameter to describe interfacial phenomena since it includes effects due to interfacial adhesive phenomena and also plastic deformation induced in the copper bar by severe contact pressures. Following the work of Challen [25], a single decomposition can be done:

$$\mu_{\mathrm{mac}} = \mu_{\mathrm{plas}} + \mu_{\mathrm{adh}} \tag{4}$$

where μ_{plas} is the plastic deformation part and μ_{adh} the interfacial adhesive part of the macroscopic friction coefficient μ_{mac} . One of the main objectives of this model is to extract, by iteration, the adhesive part of the macroscopic coefficient μ_{adh} and the heat partition ratio α so that numerical macroscopic data $\mu_{\mathrm{mac-num}}$ and $\phi_{\mathrm{pin-num}}$ fit correctly the experimental data.

A 3D ALE model implemented in Abaqus/Explicit© is used, considering a static pin and a moving work material with a sliding velocity V_{s}, the copper bar in this case. The normal force F_{n} is applied on the reference point of the pin. Convection with ambient air is neglected. A complete description of this model can be found in [24,26]. To capture important gradients occurring close to the pin/copper interface, a fine mesh size of 10μm before deformation was used.

A Johnson-Cook flow stress model [27] is used to describe mechanical behavior with parameters identified by Fang [28] for OFHC Cu and reported Table 1. Thermal and mechanical properties of Cu are presented Table 2.

$$\sigma_{eq} = [A + B\varepsilon^n]\left[1 + Cln\left(\frac{\dot{\varepsilon}}{\dot{\varepsilon}_0}\right)\right]\left[1 - \left(\frac{T - T_0}{T_F - T_0}\right)^m\right] \tag{5}$$

Table 1: Johnson-Cook constitutive model parameters

A(MPa)	B (MPa)	n	C	$\dot{\varepsilon}_0$ (s^{-1})	T_0 (°C)	T_F (°C)	m
90	292	0.31	0.025	1	25	1084	1.09

Table 2: Material properties of the Copper material

Parameter	Temperature (°C)	Value
Thermal Conductivity (W.m^{-1}.K^{-1})	28	387
	228	382
	528	366
Density (kg.m^{-3})	30	8950
Specific Heat (J.kg^{-1}.K^{-1})	28	384
	228	406
	528	431
E (GPa)	30	120
Poisson's ratio	30	0.33

4. Results

4.1. Macroscopic coefficient

According to Figure 5a, the numerical results concerning the macroscopic friction coefficients and the heat flux transmitted to the pin have good correlations with the experimental results. Values of μ_{mac} are quite similar for sliding velocities of 20 and 100m/min and are close to 0.2. For $V_s = 250$m/min, $\mu_{mac-exp} = 0.77$, reflecting a sharp increase between 100 and 250m/min. Raise of this coefficient with sliding velocity differs of many metallic alloys. Data presented in [29], obtained with the same tribometer used for the present study, show a decrease of the macroscopic friction coefficient with sliding velocity for ferrito-perlitic, martensitic and austenitic steels, Inconel and titanium alloy. Copper is known as a very malleable alloy. Moreover, friction tests with high sliding velocities create an important temperature raise at the surface. For these two reasons, the contact surface (the frontal part of the hemispherical pin) is bigger at high sliding velocities, increasing the size of the surface ploughed and finally values of friction coefficients. Figure 5 also shows that the simulated adhesive friction coefficient $\mu_{adh-num}$ represents in average 65% of $\mu_{mac-num}$. By combining Eq. (1) and (2), we obtain:

$$\phi_{pin} = \mu_{mac} F_n V_s - \phi_{copper} \tag{6}$$
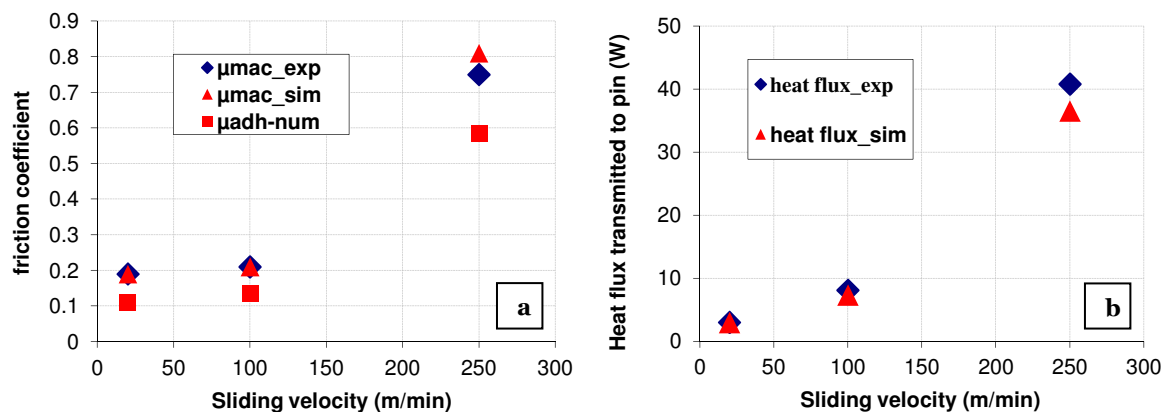

Figure 5: Evolution of (a) friction coefficients and (b) heat flux transmitted to pin versus sliding velocity. F$_n$ = 600 N.

Figure 5b confirms that the variation of ϕ_{pin} with V_s is therefore closely related to the evolution of μ_{mac} with V_s. Values of Experimental heat flux transmitted to the pin are 3W at 20 m/min, 8W at 100 m/min and 40W at 250m/min.

4.2. Microstructural evolutions

In the same way as for the macroscopic coefficients, the microstructural evolutions induced by friction tests at 20 and 100m/min are similar, and those at 250m/min are strongly different. For the lowest sliding velocities, the microstructures of the observed samples reflected a strong work-hardening (Figure 6a) in a layer of approximately 100μm depth. Locally, some fine recrystallized grains were observed (Figure 6b), within a layer of 5μm located at the extreme surface of the material. These grains have an average size of about 1μm and represented less than 5% of the extreme surface.
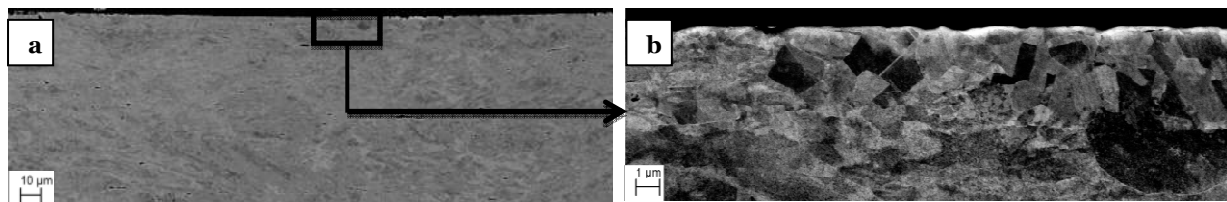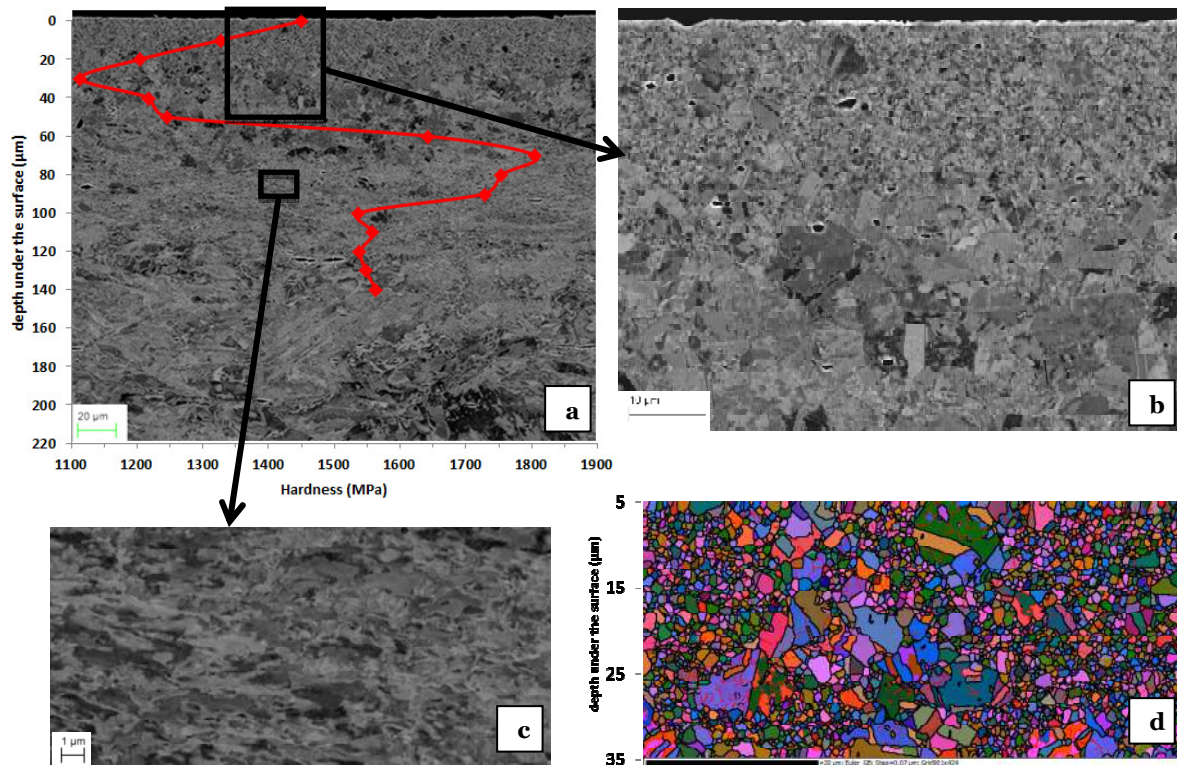

Figure 6: SEM micrographs of surface of the copper bar after a friction test with F_n = 600 N, V_s = 20m/min. (a) General view, b) detail. Sliding direction is perpendicular to the observation plane.

The microstructures obtained with a sliding velocity of 250m/min are presented Figure 7. First of all, an important microstructure gradient can be seen in function of depth (Figure 7a). Between 0 and approximately 25μm under the surface, fine recrystallized grains are visible with dispersion a few large recrystallized grains (top of Figure 7b). More than 95% of the surface is recrystallized and the average grain size, estimated by EBSD (Figure 7d), is about 700nm. This map also shows that global texture of these fine recrystallized grains is weak. A second layer is then identifiable, between about 25 and 60μm under the surface (bottom of Figure 7b). It is partially recrystallized, between 50% and 75%, with much larger grains than in the first layer, some of them being larger than 10μm. The dominant microstructure is then "large" recrystallized grains, with dispersion of both fine recrystallized grains and work-hardened areas. Moreover, growth twins are visible. These large grains and growth twins are evidences of post-dynamic evolution in the material. Under this second layer, no recrystallized grains are visible. Deformation and work-hardening received by the initial grains decrease with depth. In fact grains are much more fragmented 90μm under the surface (Figure 7c) than 200μm (bottom of Figure 7a).

Figure 7a also shows a good correlation between microstructure and hardness evolutions. Between 150μm and 100μm, hardness is constant, around 1550MPa, meaning that the level of work-hardening is similar. Then, hardness increases sharply until 1800MPa at 70μm under the surface, which is consistent with the fact that the more the surface is close, the more work-hardening is important. Then, harness decreases until 30μm due to the fact that dislocation-free recrystallized grains are present. Value of hardness is higher at 30μm than at 60μm because of a highest recrystallized fraction. Then, in the first layer presented previously, rise of hardness is mainly due to an effect of the grain size. Indeed, a relation between yield stress and grain size is described mathematically by the Hall−Petch equation:

$$\sigma_y = \sigma_0 + \frac{k}{\sqrt{d}} \tag{7}$$

where σ_y is the yield stress, σ_o is the friction stress when dislocations move on the slip plane, k is the strengthening coefficient, and d is the average grain diameter.

Figure 7: (a) SEM micrograph of the surface of the copper bar + curve showing evolution of hardness versus depth under the surface after a friction test with F_n = 600N, V_s = 250m/min. (b) and (c) are details of (a). (d) EBSD map between 5 and 35µm under the surface showing Euler angles + grain boundaries misorientation angles (θ). Black lines: θ> 15°, red lines: 2°<θ< 15°. Sliding direction is perpendicular to the observation plane.

4.3. Numerical results

Figure 8 and Figure 9 present profiles of some local parameters, temperature and equivalent strain, obtained with a respective sliding velocity of 100 and 250m/min. First of all, each figure shows that maximum values are associated with the interface between the copper bar and the pin. Comparison between these two figures underlines the importance of sliding speed on local thermomechanical conditions of deformation. Maximum temperature rises are around 100°C at 100m/min, and 400°C at 250m/min. Maximum equivalent strains are approximately and respectively 0.6 and 10. Strain rate maps, not reproduced here, are also sharply different. Maximum values are around 10000s^{-1} close to the surface at 250m/min, which is an order of magnitude higher than at 100m/min.

Due to highest maximum values, gradients of these local parameters with depth are more pronounced at 250m/min than at 100m/min. Deformation is then more homogeneous with

depth for tests performed at 20 and 100m/min and can be considered as cold, fast and quite small, in term of strain, deformation. At 250m/min, temperature reaches a value higher than 300°C, and equivalent strains are over 2, in a layer of 60μm where recrystallization phenomena are observed. Deformation can be qualified as warm/hot severe plastic deformation.
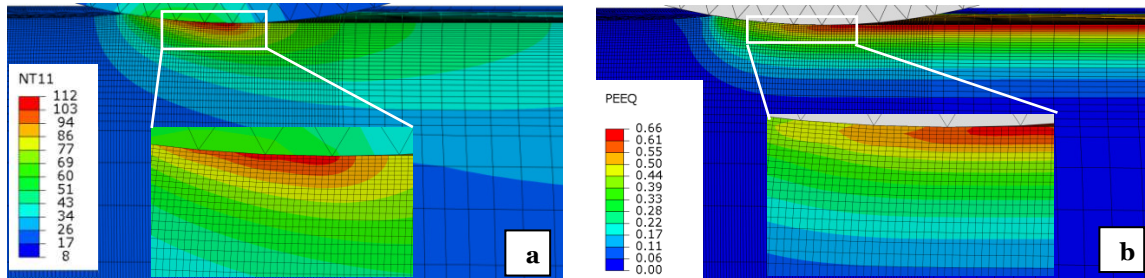

Figure 8: Profiles of local parameters for $F_n = 600N$ N and $V_s = 100m/min$. General view and detail for (a) temperature, (b) equivalent strain.
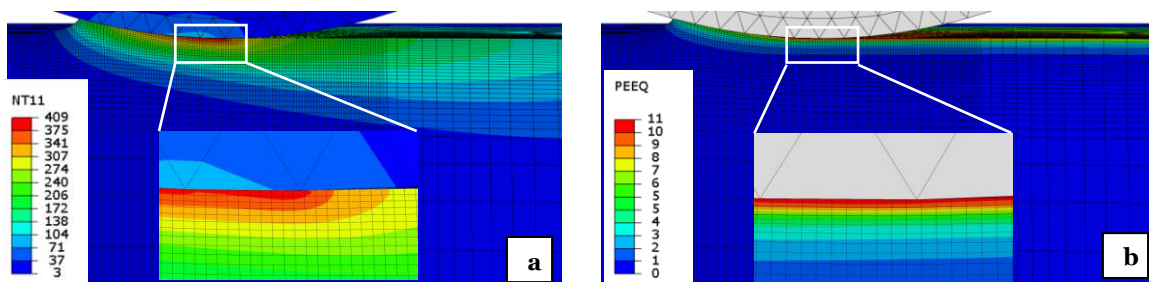

Figure 9: Profiles of local parameters for $F_n = 600N$ and $V_s = 250m/min$. General view and detail for (a) temperature, (b) equivalent strain.

In order to understand differences of microstructures between the first and the second layers exposed in part 4.1, evolutions of equivalent strain and temperature versus time have been plotted at 10μm and 50μm under the surface (Figure 10). These curves show firstly that amounts of deformation received for these two depths are sharply different, ε > 9 and ε < 3 at respectively 10μm and 50μm under the surface (Figure 10a). Concerning thermal histories, one can see on that maximum temperature reached at 50μm is approximately 300°C, which is about 100°C less than at 10μm. Moreover, the gap between the two profiles of temperature after peaks of temperature, and thus after deformation, becomes quickly negligible, due to the fact that copper has a very high thermal conductivity.
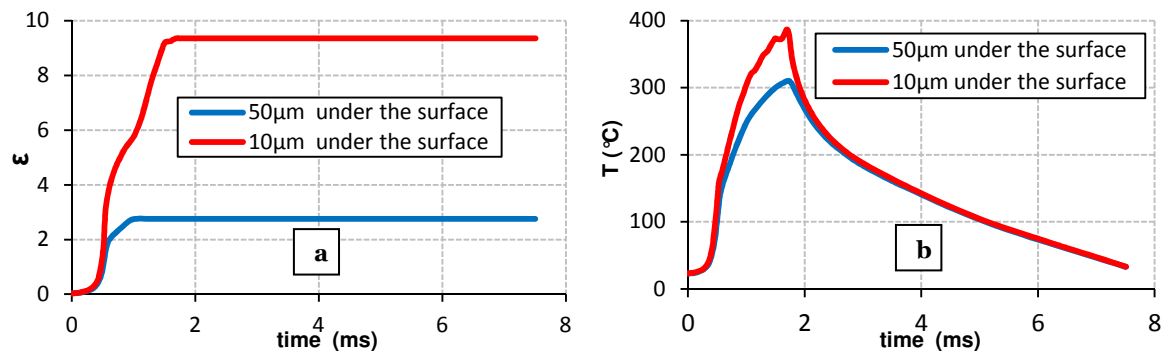
Figure 10: Local evolutions of equivalent strain (a) and temperature (b) versus time for $F_n = 600N$ and $V_s = 250m/min$.

4. Discussion

Microstructures generated by friction tests performed at sliding velocities of 20 and 100m/min do not exhibit significant recrystallization, whatever the depth under the surface is. Numerical simulations show that the heat flux transmitted to the copper bar is not sufficient to generate important temperature rises, peaks of temperature being approximately 100°C. Friction tests, for these velocities, can be considered as cold working and even if copper is submitted to severe plastic deformation in terms of contact pressure, equivalent strains induced at these sliding velocities are not sufficient enough to generate a new population of recrystallized grains. In fact, at low temperatures and for materials with low stacking fault energy such as copper, high levels of deformation are expected to create new grains by fragmentation of initials grains. This type of mechanism, called continuous dynamic recrystallization (CDRX) [30], transformed in a progressive way, by accumulation of dislocations, sub-boundaries in grain boundaries. Contrary to the results exposed in [21] for large deformations of Cu, conditions of deformation do not permit the microstructure to reorganize itself and form new grains, and then high work-hardened material is obtained under the pin/copper interface.

Contrary to tests performed at lower sliding velocities, significant recrystallization phenomena are observed at 250m/min. The friction coefficients, particularly the adhesive part, and also the heat flux transmitted to the copper bar are much more important than for lower sliding speed. Close to the surface, equivalent strain is high, temperature reaches 400°C leading to a ratio $T_{max}/T_f = 0.5$ (in Kelvin) which is the usual value to define the border between hot and warm/cold deformation. Moreover, global texture of recrystallized grains is weak. These observations suggest that discontinuous dynamic recrystallization (DDRX) [19] happens for this sliding velocity, which is the mechanism of recrystallization expected during hot working. In fact, contrary to CDRX, DDRX consists in nucleation and growth of new grains. The texture of these new grains is not related to the texture of the deformed initial grains, as in CDRX, leading to a weak texture, which is the case here.

Differences in microstructures have been observed in function of depth under the surface. To sum up, close to the surface (first layer) recrystallized grains are fine and recrystallization is complete. In the second layer, recrystallization is well advanced but not achieved, with significant presence of large grains, interpreted as post-dynamic grain growth. Conditions of deformation (strain, stress, temperature, strain rate) can explain these differences. In the first layer, these conditions lead to a nucleation frequency of germs sufficiently high to generate a homogeneous layer of small recrystallized grains. These grains

are all dislocations free and do not have significant differences in terms of size. Thus, they are no driving forces for grain growth after deformation. On the other hand, in the second layer, less severe plastic deformation conditions lead to a smaller nucleation frequency. After deformation, the microstructure is composed both by work-hardened areas and new recrystallized grains. Contrary to the first layer, a strong difference in dislocations density exists between a recrystallized grain and work-hardened copper, which forms the driving force that can promote grain growth for a part of the recrystallized grains at the expense of work-hardened areas, leading to the presence of the observed large grains.

5. Conclusion

Effect of sliding velocity on friction-induced microstructural evolution in copper test has been investigated by means of microstructural observations and numerical simulations. It has been shown that:
- the macroscopic coefficients and local parameters extracted from the numerical model are very sensitive to sliding velocity.
- work-hardened material was obtained at low sliding velocity whereas recrystallization occurred for the highest value of V_s.
- an increase of sliding velocity generates in particular a higher deformation and a temperature rise which promote the evolution of the microstructure by discontinuous dynamic recrystallization.
- good correlation between hardness and microstructure has been identified.

To conclude, a simple test with a particular tribometer, combined with numerical simulations, permitted to simulate contact conditions occurring during machining processes and to extract evolutions of local parameters. Differences of microstructure modifications induced by a change of sliding velocity can be justified by the knowledge of these local variables.

6. Acknowledgement

References

[1] Novovic D, Dewes RC, Aspinwall DK, Voice W and Bowen P 2004 *Int. J. Mach. Tool Manu.* **44** pp 125-134
[2] Ulutan D and Ozel T 2011 *Int. J. Mach. Tool Manu.* **51** pp 250-280
[3] Chomienne V, Verdu C, Rech J and Valiorgue F 2013 *Procedia Engineering* **66** pp 274-281
[4] Valiorgue F, Rech J, Hamdi H, Gilles P and Bergheau JM 2012 *Int. J. Mach. Tool Manu.* **53** pp 77-90
[5] Mondelin A, Valiorgue F, Rech J, Corret M and Feularch E 2012 *Int. J. Mach. Tool Manu.* **58** pp 69-85

[6] Arrazola PJ, Kortabarria A, Madriaga A, Esnaola JA, Fernandez E, Cappelini C, Ulutan D and Ozel T 2014 *Simul. Model. Pract. Th.* **41** pp 87-103

[7] De PS, Mishra RS and Smith CB 2009 *Scripta Mater.* **60** pp 500-503

[8] Chan KS 2010 *Int. J. Fatigue* **32** pp 1428-1447

[9] Humbertjean A and Beck T 2013 *Int. J. Fatigue* **53** pp 67-74

[10] Ding H, Shen N and Shin YC 2011 *Comp Mater Sci* **50** pp 3016-3025

[11] Mondelin A, Valiorgue F, Rech J, Corret M and Feularch E 2013 *Procedia CIRP* **8** pp 311-315

[12] Claudin C, Mondelin A, Rech J and Fromentin G 2013 *Int. J. Mach. Tool Manu.* **50** pp 681-688

[13] Gravier J 2009 *Thesis* Impact de l'usinage de superfinition sur la zone affectée par le procédé Université de Bourgogne

[14] Bissey-Breton S, Gravier J and Vignal V 2011 *Procedia Engineering* **19** pp 28-33

[15] Suresh KS, Sinha S, Chaudhary A and Suwas S 2012 *Mater Charact* **70** pp 74-82

[16] Belyakov A, Gao W, Miura H and Tsuzaki K 1998 *Metall. Mater. Trans. A* **29A** pp 2957-2965

[17] Swaminathan S, Brown TL, Chandrasekar S, McNelleya TR and Compton WD 2007 *Scripta Mater* **56** pp 1047-1050

[18] Ni H, Elmadagli M and Alpas AT 2004 *Mater Sci Eng A* **385** pp 267-278

[19] Humphreys FJ and Hatherly M 2002 *Recrystallization and Related Annealing Phenomena* Ed. Elsevier

[20] Sakai T, Beliakov A, Kaibyshev R, Miura H, Jonas JJ 2014 *Prog. Mater. Sci.* **60** pp 130-207

[21] Beliakov A, Miura H and Sakai T 2001 *Phil. Mag.* A **81** pp 2629-2643

[22] Bonnet C, Valiorgue F, Rech J, Claudin C, Hamdi H, Bergheau JM and Gilles P 2008 *Int. J. Mach. Tool Manu.* **48** pp 1211-1223

[23] Zemzemi F, Rech J, Ben Salem W, Dogui A and Kapsa P 2009 *J. Mater. Process. Tech.* **209** pp 3978-3990

[24] Courbon C 2011 *Thesis* Vers une modélisation physique de la coupe des aciers spéciaux : intégration du comportement métallurgique et des phénomènes tribologiques et thermiques aux interfaces Université de Bourgogne

[25] Challen JM and Oxley PLB 1979 *Wear* **53** pp 229-243

[26] Ben Abdelali H, Courbon C, Rech J, Ben Salem W, Dogui A and Kapsa P 2011 *J. Trib.* **133**

[27] Johnson GR and Cook WH, 1983 Proceedings of the Seventh International Symposium on Ballistics (Hague, Netherlands) pp. 541–547.

[28] Fang N 2005 *J. Eng. Mater. Tech.* **127** pp 192–196.

[29] Rech J, Arrazola PJ, Claudin C, Courbon C, Pusavec F and Kopac J 2013 *Cirp. Ann.-Manuf. Techn.* **62** pp 79-82

[30] Gourdet S and Montheillet F 2003 *Acta Mater.* **51** pp 2685-2699